STUDIES ON THE ICE CAP OF GALINDEZ ISLAND, ARGENTINE ISLANDS

By R. H. THOMAS

ABSTRACT. Most of the Argentine Islands support ice caps which are considerably larger than would be expected to exist on such small islands. These are thought to be relics of the former coastal ice shelf which are nourished by large accumulations of drift snow; this is a consequence of the prevailing north-north-east wind combined with high rocky cliffs above the northern coasts which act as drift obstacles. It is deduced that over a number of years the budget state of the Galindez Island ice cap is one of equilibrium with minor oscillations in surface level related approximately to the cyclic variations in the annual mean temperature.

Surface movement over the ice cap is negligible except in the ice adjacent to the southern ice cliffs. This active ice receives a high net accumulation of snow which is balanced by forward movement and periodic calving at the ice cliffs. It is suggested that the surface movement observed is caused by plastic deformation of the underlying ice which is possibly warmed by geothermal heat and heat received from the sea. The possibility of bottom sliding is examined and it is considered unlikely to be the only mechanism involved.

DURING the period 1960–62, observations were made on the Galindez Island ice cap, one of several small ice caps which exist on many of the Argentine Islands, a group of small islands about 7 km. west of the Graham Land peninsula at lat. 65°15′S., long. 64°17′W. (Figs. 1 and 2). These islands are recognized as being *roche moutonnées* with their stoll ends pointing north; originally their ice caps were relics of the coastal ice shelf which eroded the islands to their present form. The shape of the ice caps has subsequently been modified by:

i. Preferential ablation on the northern coasts.
ii. Rock shape.
iii. Wind direction.

Thus, the islands now possess rocky northern coasts, rising steeply to a rock peak, to the south of which lies the bulk of the ice cover, in the form of a large drift structure with its axis of symmetry coincident with the direction of the prevailing north-north-east wind.

Galindez Island measures about 1,100 m. from east to west and about 700 m. from north to south, whilst the ice cap (Fig. 3) is about 400 m. square and is situated to the south of the rock peak which is at a height of 50 m.

OBSERVATIONS AND METHODS

Measurements of accumulation and ablation were made using a network of stakes which also served as movement markers. These stakes were established 100 m. apart in a roughly rectangular pattern during June 1960 (Fig. 2). Both aluminium and ramin wood stakes of lengths from 2·4 to 3·4 m. were used and wherever possible they were drilled 0·5 m. into the underlying ice and set vertically. In all other cases the base of each stake was frozen into a thick ice layer.

Budget

At intervals throughout 1960–62 core samples were taken from the snow cover at each stake site down to a reference horizon (the surface of the ice into which the stake was anchored). These samples were weighed and the results (Fig. 4) give an indication of the net surface accumulation during the period.

The samples were taken with an aluminium tube of 6 cm.^{2} cross-section, and 1 to 3 m. in length, depending on the length of core required. To obtain a core, the tube was sunk (if necessary with the aid of a mallet) to the depth of the ice surface and driven about 1 cm. into the ice. It was then raised complete with core, which was retained, partly by friction against the walls of the tube, and partly by the disc of ice removed from the ice surface and jammed into the end of the tube. The tube was weighed when empty, and again when full of snow; at least three samples were taken near each stake. Since the level of the ice surface

often changed as a result of the accumulation of superimposed ice, a correction was made for such accumulation by assuming its density to be 0·8 g. cm.$^{-3}$.

A Büchart silicone-damped balance which had been modified to weigh up to 2,000 g. was used for all weighings. This is a bulky and fragile instrument, and it is virtually impossible to use in winds of a velocity greater than 5 m./sec. Because of its unreliable behaviour all

Fig. 1. Aerial photograph of the south-eastern part of the Argentine Islands. December 1956.

weighings were checked against standard weights and therefore rendered accurate to within ±10 g.

In Fig. 4 the weight of snow per cm.^{2} above a fixed horizon is plotted against time for several representative stakes. The snow depth above the same horizon is also plotted for these stakes in order to assess the value of such measurements. Although the two sets of graphs follow the same general form, the snow depth does not give a true indication of snow mass. This is due to variations in the snow density with the season and the position of the sampling

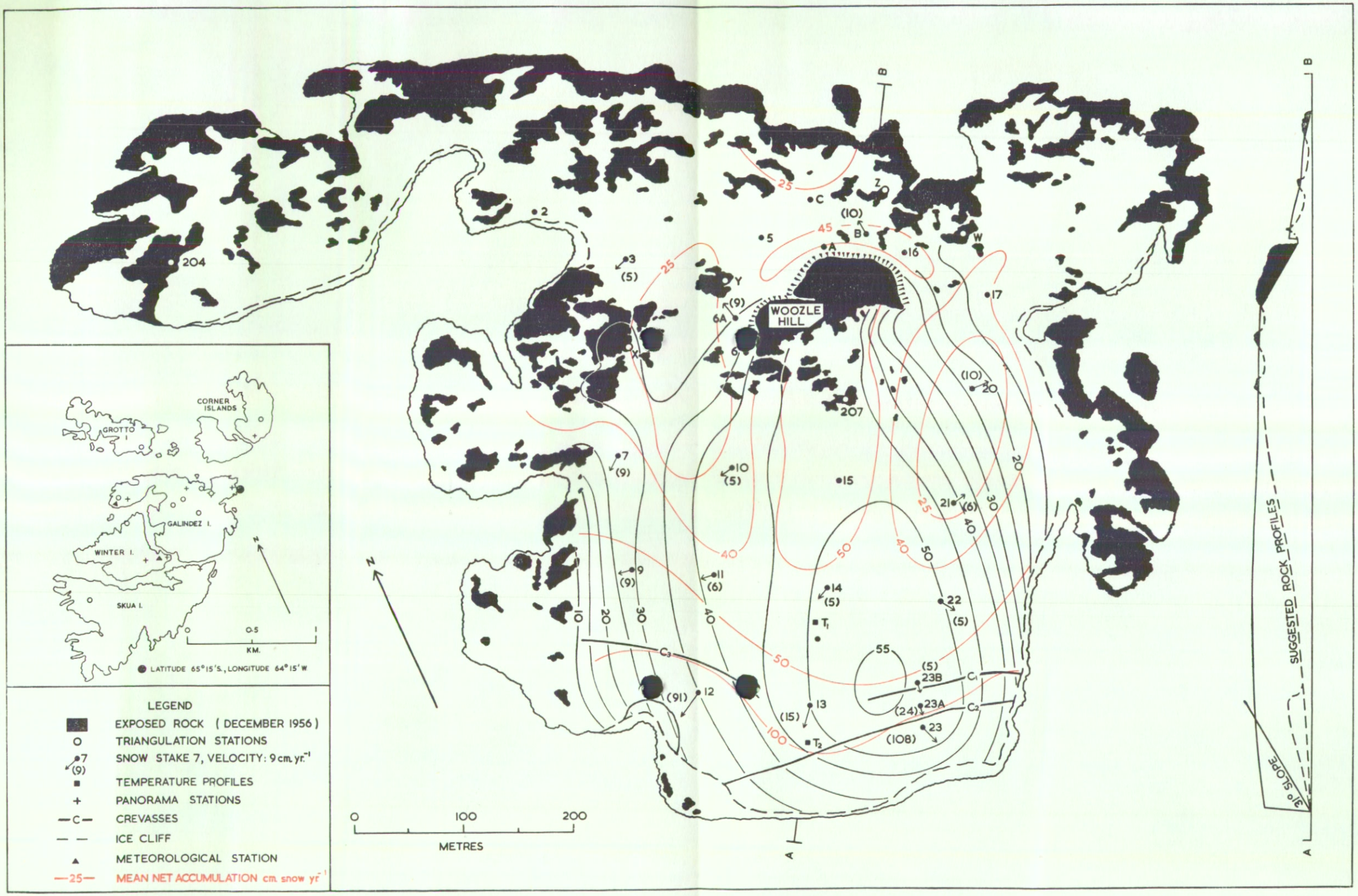

Fig. 2. Map of Galindez Island showing exposed rock in December 1956, snow contours at 5 m. intervals in March 1961, major crevasses, positions at which snow temperatures were measured, stake positions, annual surface movement, and overprinted in red the distribution of net accumulation during the two budget years March 1961–March 1963. On the section AB two suggested rock profiles are shown. The inset is a map of the islands in the immediate vicinity of Galindez Island, showing the positions of rock triangulation stations, and the stations from which panoramas of Galindez Island were taken in March and April 1961.

[face page 28

site (Fig. 5). However, useful results can be obtained by comparing snow depths at the end of consecutive budget years and, knowing the density of the snow at the stake site throughout this period, converting the respective measurements into their water equivalents. This assumes that the snow density is the same at the end of each budget year, which is unlikely to be true for years with low summer temperatures and relatively little ablation. However, measurements taken over a number of years should give a reasonably accurate picture of the budget state.

Panoramas of Galindez Island were taken at the end of the budget year 1960–61 (March 1961) from the positions shown in Fig. 2. It is planned that this procedure should be repeated at the end of each budget year, thus recording any major changes in snow level over a number of years.

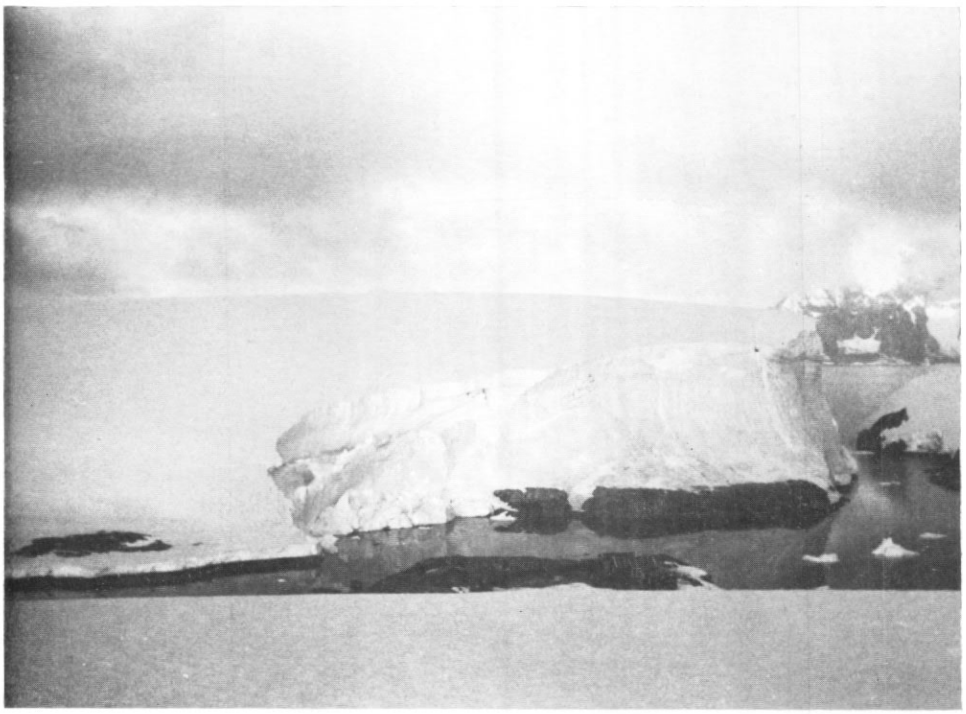

Fig. 3. The small ice cap of Galindez Island viewed from the top of Winter Island. 18 March 1961.

Movement

A network of stations on rock was established on, and near to, Galindez Island and these were tied into the existing network of British Graham Land Expedition stations, whose rectangular coordinates were known. From these stations the snow stakes were observed in April/May 1961, December/January 1962 and January 1963, using a Tavistock theodolite. Sightings were made on to the top of each stake but at many of the stakes little or no vertical movement was observed; this was an indication that, where vertical movement was observed, it was due to downward motion of the ice, and not to sinking of the stakes within the ice. Wherever possible, each stake was observed from at least three rock stations, two readings being obtained at each station. Using the line from station 207 to station 204 (Fig. 2) as base line, and station 207 as the origin, the polar coordinates of all stakes were calculated. In most cases two or three independent triangles were used in the calculation of each stake position and the values thus obtained were found to agree to within ± 2 cm. As a further check on the movement of stake 23, the distances between stakes 23, 23A and 23B were

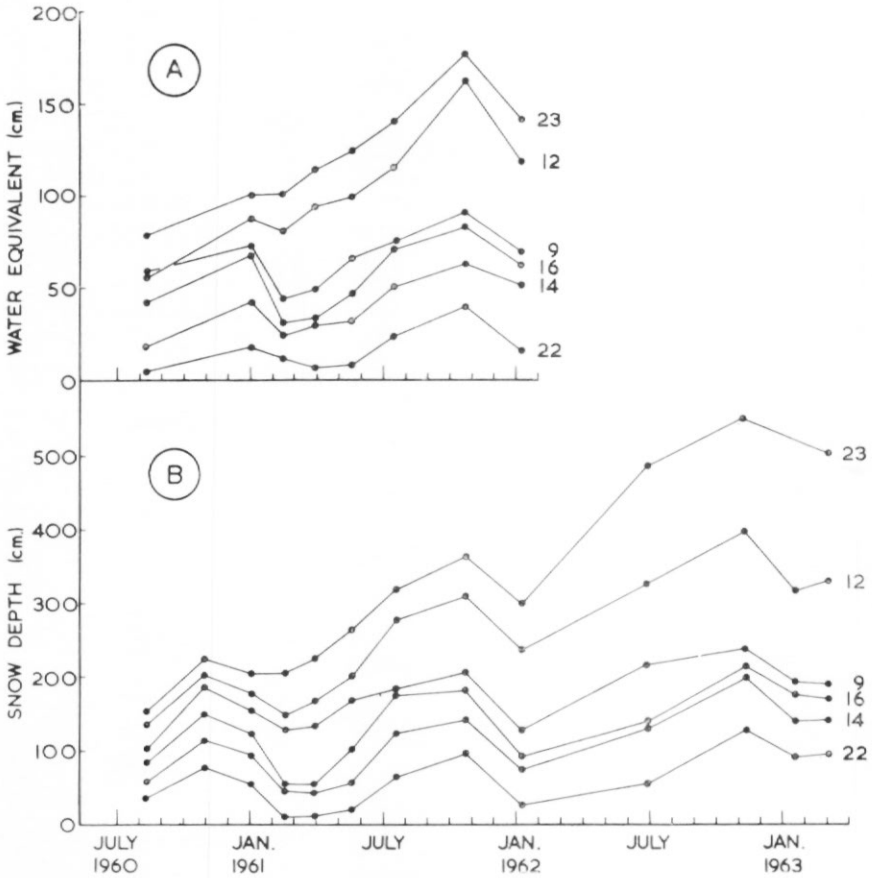

Fig. 4. A. The change in snow mass on the Galindez Island ice cap during the period August 1960–January 1962.

B. The change in the depth of surface snow on the Galindez Island ice cap during the period August 1960–March 1963.

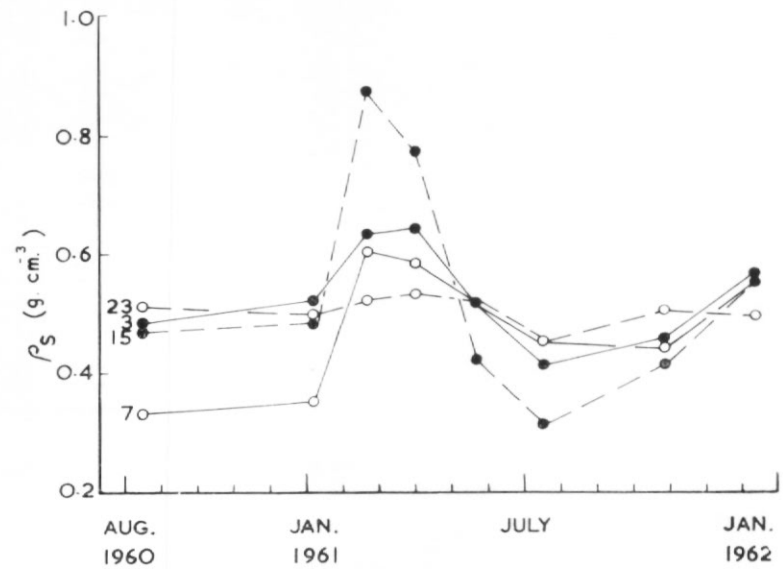

Fig. 5. The seasonal variation in surface snow density at stakes 3, 7, 15 and 23 on the Galindez Island ice cap for the period August 1960–January 1962.

accurately taped in March 1961 and January 1962. The movement of stake 23 thus measured agreed to within 5 cm. with that observed by theodolite.

The polar coordinates of the stakes in April/May 1961 and the movements observed subsequently are given in Table I, and expressed graphically on the map in Fig. 2. This map was drawn from existing air photographs on which it was possible to identify the rock

TABLE I. STAKE POSITIONS ON GALINDEZ ISLAND IN APRIL 1961 AND SUBSEQUENT MOVEMENT

Stake Number	*Position in April 1961*			*Movement: April 1961–January 1962* (cm.)		*Approximate Movement: January 1962–January 1963* (cm.)		*Movement in One Year* (cm.)	
	R	*H*	*θ*	*Horizontal*	*Vertical*	*Horizontal*	*Vertical*	*Horizontal*	*Vertical*
	(cm.)	(cm.)							
2	32,020	1,095	340°44′38″	Nil	Nil			Nil	Nil
3	23,025	1,937	339°02′45″	+4	Nil			+5	Nil
5	16,021	2,110	309°05′20″	Nil	Nil			Nil	Nil
6A	12,100	3,190	335°10′20″	+7	Nil			+9	Nil
7	20,632	2,867	025°05′19″	+7	−3			+9	−5
9	23,976	2,993	049°46′26″	+7	−3	+8	−3	+9	−4
10	11,630	4,336	042°00′10″	+4	Nil			+5	Nil
11	19,219	4,331	064°28′48″	+4	Nil	+4	Nil	+6	Nil
12	28,777	3,645	074°45′22″	+65	−45			+91	−63
13	26,975	5,165	094°54′20″	+11	−6	+13	−5	+15	−8
14	16,619	5,311	096°16′08″	+3	Nil	+4	Nil	+5	Nil
15	7,124	5,080	094°44′04″	Nil	Nil			Nil	Nil
16	13,825	2,067	259°37′58″	Nil	Nil			Nil	Nil
17	15,453	1,387	227°45′32″	Nil	Nil			Nil	Nil
20	11,208	2,682	196°18′18″	+7	Nil			+10	Nil
21	13,215	4,332	148°08′28″	+5	Nil			+6	Nil
22	19,637	5,178	127°14′08″	+3	Nil	+5	Nil	+5	Nil
23	29,666	5,425	115°18′34″	+77	−63			+108	−88
23A	27,794	5,524	115°34′10″	+17	−5	+20	−6	+24	−7
23B	25,726	5,563	115°54′06″	+3	Nil	+7	−3	+5	−3
A	13,464	2,136	289°24′08″	Nil	Nil			Nil	Nil
B	14,595	2,133	274°11′58″	+7	Nil			+10	Nil
C	17,771	1,499	291°28′48″	Nil	Nil			Nil	Nil

Position is (R, H, θ), where R = distance from station 207 to the stake, H = height above sea-level, and θ = the horizontal angle between stations 204, 207 and the stake read anti-clockwise (station 207 is the origin of the coordinate system).

stations used for the movement observations. It has therefore been possible to mark accurately the stake positions and, using their known heights as spot heights, to insert contour lines at 5 m. intervals for the period April/May 1961.

Weather

Meteorological observations were made at the Argentine Islands in 1935 by the British Graham Land Expedition and from 1947 to the present time by the Falkland Islands Dependencies Survey and the British Antarctic Survey. Observations prior to early 1954 were made at the old station on Winter Island (Fig. 2), but since then they have been made at the new station on Galindez Island.

Unfortunately no reliable means of measuring the amount of snow precipitation has yet been devised and accurate figures for this important variable are not available. However, work being done now at the Argentine Islands by A. Schärer, using a large snow gauge containing an anti-freeze liquid and set about 4 m. above the snow level, should produce useful results.

Temperatures in the snow

From March to December 1961 snow temperatures were measured at depths of 0·5, 1·0, 2·0, 4·0 and 8·0 m. below the 1961 summer surface at two points on the ice cap (T_1 and T_2 in Fig. 2). The 8 m. holes were made with a drilling device, and Stantel resistance thermistors were used in conjunction with a Post Office box for temperature measurements.

The thermistors were calibrated against a standard National Physical Laboratory tested alcohol-in-glass thermometer; they were strapped in groups of three to the thermometer so that the resistance units were alongside the thermometer bulb. This device was immersed in paraffin surrounded by a mixture of snow and calcium chloride, sufficient paraffin being used to ensure a slow cooling rate. The initial temperature of the paraffin was +5° C, and this was lowered to −25° C, whilst the paraffin was stirred continuously. Readings of each thermistor were taken at intervals of 1° C, the resistance being measured at the same time as the thermometer was read.

To correct for the cooling time-lag of the alcohol thermometer, the calibration was repeated whilst the paraffin warmed to room temperature. In fact, very little time-lag was observed due to the slow cooling rate. In an initial attempt to calibrate the thermistors, it was found that at constant temperature it was impossible to obtain a steady value for the resistance, and this was presumed to be due to heating of the resistance wire by current from the Post Office box. In order to overcome this, a standard resistance (calibrated for changes in temperature) was connected in series with the thermistor, thus lowering the current and reducing the heating effect.

After calibration, one terminal of each thermistor was connected at the required intervals to a common insulated copper wire lead. The other terminal was connected to a clearly labelled independent lead of the appropriate length. The resistance of a known length of copper wire was measured and the result indicated that the maximum error introduced by the leads was less than 0·1° C. All connections were soldered and insulated with Bostik adhesive and insulating tape, while the glass thermistors were sealed into short lengths of Tufnol tubing.

When they had been finally connected, the thermistors were checked at several points on their calibration curves to ensure that these had not altered. They were then lowered down the 8 m. drill hole, the bottom thermistor being weighted to facilitate a smooth descent. Near the hole a small watertight terminal box was bolted to snow stakes in such a manner that it was capable of being raised or lowered to suit the snow level.

The thermistors were finally checked *in situ* against a standard thermometer lowered down the drill hole to the appropriate depth, and allowed to remain in position for 10 to 15 min. in order to assume the temperature of its surroundings. Thermistor readings were found to agree to within less than 0·5° C with those obtained from the thermometer. The thermistors at site T_1 (Fig. 2) were in solid ice and the drill hole was filled with water to seal it; those at site T_2 were in firn and the hole was accordingly filled with snow. Temperature readings

were made at both sites from March to November 1961, and the results obtained are illustrated in Fig. 6.

Interpretation of Results and Discussion

Sources of accumulation

a. *Snow deposition (including drift and all solid water forms).* During the accumulation season (March/April to October/November) the gross accumulation is normally large, and falling snow is usually accompanied by a strong wind. The resultant accumulation is much

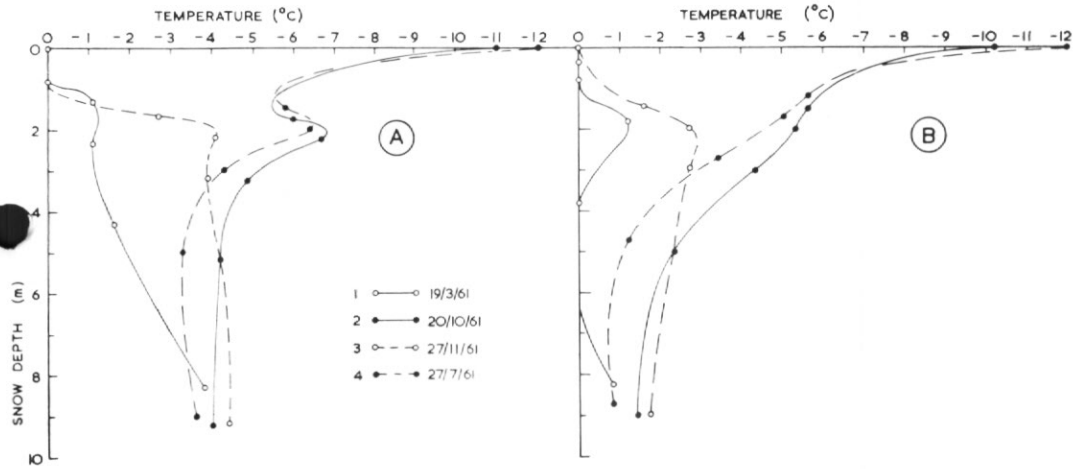

Fig. 6. Temperature profiles in the ice cap of Galindez Island measured on 19 March, 27 July, 20 October and 27 November 1961.

A. Measurements in ice at point T_1 (Fig. 2).

B. Measurements in firn at point T_2 (Fig. 2).

affected by the direction and temperature of this wind. From the wind frequency chart in Fig. 7 it can be seen that there are two main snow-bearing winds:

i. North-north-east. This is the prevailing wind at the Argentine Islands; it is a warm wind, bringing coarse-grained wet snow and air temperatures of $-2°$ C to $+8°$ C which cause, even during the winter, rapid surface thawing. Drift patterns in the lee of obstacles are to a certain extent protected from wind erosion, initially because the snow of which they are composed is wet and adhesive, and later by the formation of thick icy crusts.

ii. South-west. This is a cold wind bringing fine-grained, dry snow which is easily drifted unless it is sufficiently protected by an overlying wind or radiation crust formed during the calm clear weather which often follows this wind.
Occasionally as much as 1 m. of light, loosely packed snow is deposited during calm conditions, but it is almost always eroded and redistributed by the first strong wind (usually from the north-north-east).

b. *Rain.* Rain is not uncommon and can affect the regime in two ways:

i. Rain falling in summer saturates and warms the snow, thus aiding sub-surface run-off.

ii. Winter rain, apart from contributing to the net accumulation, compacts the dry winter snow and, on freezing, forms a protective crust.

c. *Sublimation deposits.* During periods of high relative humidity and clear skies in late winter and early spring there is a considerable accumulation of surface hoar (leaf snow) and rime, which is usually removed by wind erosion. However, when they form during the

frequent cold clear nights of early spring, these coarse-grained arien deposits possessing a high albedo are extremely effective in protecting the underlying snow from daytime radiation. Hence, by delaying the spring melting, these deposits contribute indirectly to the net accumulation.

Agents of ablation

a. *Wind and drift erosion.* During and immediately after precipitation, much of the gross accumulation is removed by wind. Some of this snow, however, is redeposited in more

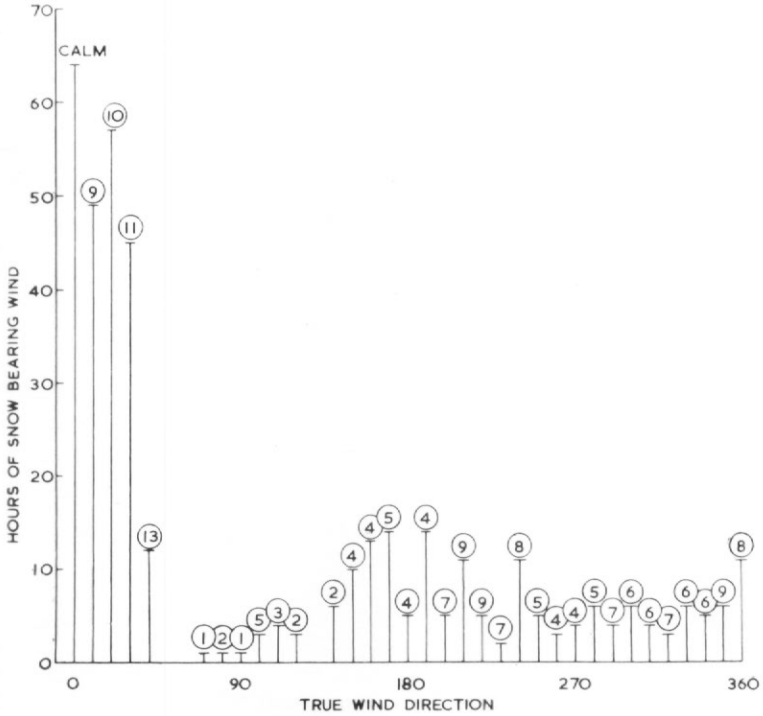

Fig. 7. The frequency of snow-bearing winds from all directions at the Argentine Islands during the period 1 April–26 October 1961. The mean wind velocity (in m./sec.) for each direction is given in a circle on the graphs.

sheltered areas. Prolonged drift erosion is responsible for the weakening and ultimate removal of surface crusts due to the cutting action of the drift particles. But this is not a frequent occurrence at the Argentine Islands.

b. *Melting of the surface snow.* In Fig. 8 the mean rate of net surface accumulation (A) is compared with several meteorological variables for a number of shorter periods (t_i) during 1960–62. The curves which most closely follow that of A are those which give a measure of the frequency of air temperatures in excess of 0° C (B and C in Fig. 8). At the Argentine Islands such temperatures are usually accompanied by low stratiform cloud, conditions which encourage rapid melting of the surface snow. Thus, the rate of net accumulation (and consequently the annual budget) is largely determined by the intensity of ablation, and not by the gross accumulation (represented by E in Fig. 8).

The rate of melting during warm sunny weather is mainly dependent on the relative humidity and the albedo of the snow. If the relative humidity is low, then the heat absorbed by the snow causes evaporation but, if it is high, then the snow melts. During spring, when the snow albedo is high, surface melting is small and is refrozen at night to produce a strong crust.

The effect is therefore a densification rather than a loss of surface snow. Later in the year, however, as the accumulated dust (diatoms, salt from sea spray and probably a large proportion of exhaust carbon from the Diesel generator at the nearby station) becomes concentrated at the surface, the albedo is considerably lowered and melting is consequently rapid, resulting finally in direct run-off of the melt water.

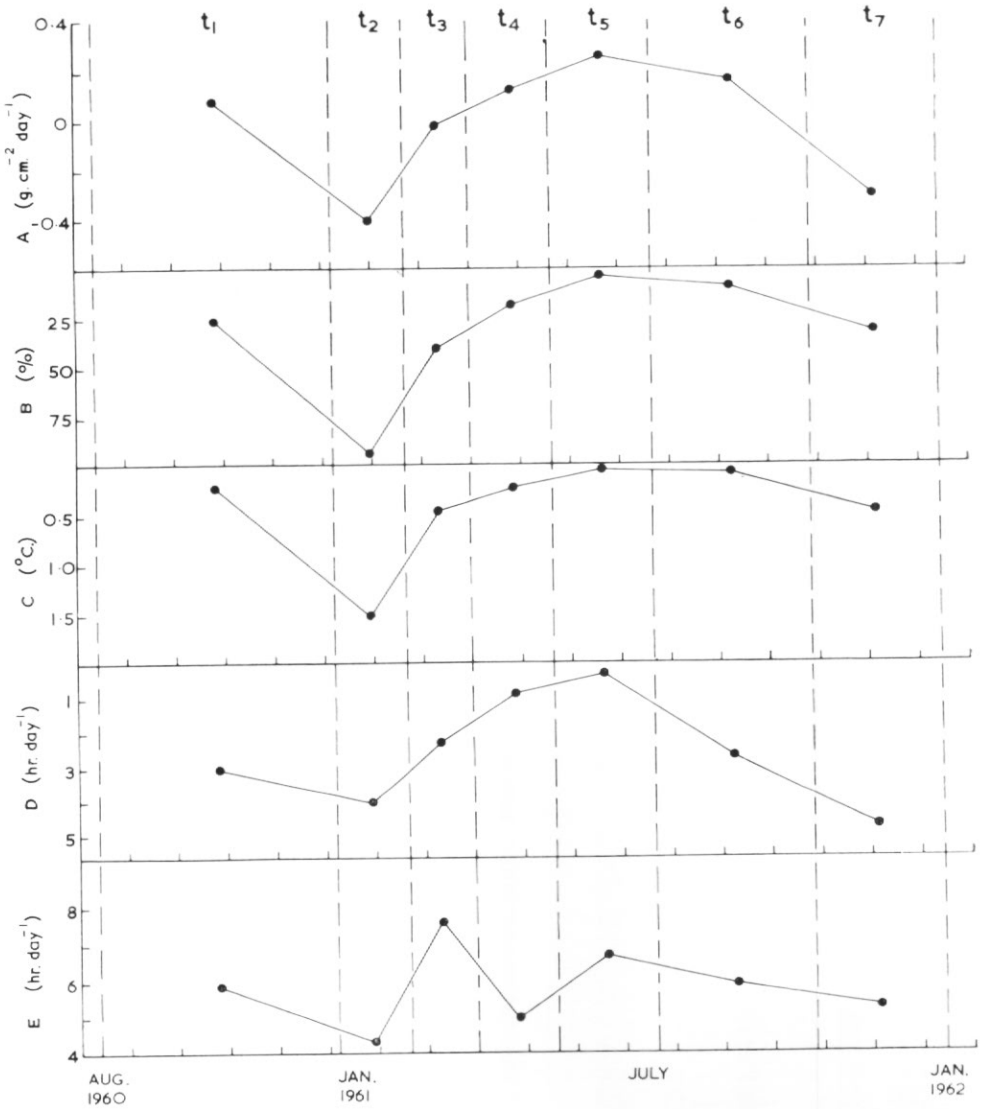

Fig. 8. Summary of meteorological observations at the Argentine Islands for the period August 1960–January 1962, which is subdivided by the vertical pecked lines on the graph into shorter periods, t_i, where $i = 1$–7.
A. The mean rate of net accumulation measured over each period t_i.
B. The percentage of each period t_i with temperatures in excess of 0° C and low stratiform cloud.
C. $\Sigma T_x/N$, where T_x = temperatures above 0° C, and N = total number of observations during each period t_i.
D. The mean duration of sunshine during each period t_i.
E. The mean duration of falling snow during each period t_i.

Density changes in the surface snow during 1960–62 are shown in Fig. 5 and its rapid increase during the summer is well illustrated. Most of the stakes are set in solid ice, and in summer the accumulation of the winter is transformed into slush and superimposed ice with an average density of 0·7 g. cm.$^{-3}$. Run-off flows along the ice surface to collect in the small gullies and form gushers at intervals along the coast. In contrast, stakes 12 and 23 are frozen into ice layers in positions where the annual net accumulation is high and solid ice is at a considerable depth. Melt water is able to penetrate to a depth of about 6 m. and therefore the density changes at stakes 12 and 23 are not so marked as at the other stake sites. Run-off consequently escapes into the numerous cracks to emerge from the ice cliffs high above sea-level, and hence cannot be confused with water produced by bottom melting.

c. *Melting at the ice/rock interface.* The rock beneath the ice is heated by:

i. Conduction of heat from exposed rock, which absorbs the sun's radiation. This causes extensive sub-surface melting near exposed rocks and mainly above the northern coast of Galindez Island.

ii. Conduction of heat from the sea. It is unlikely that this causes appreciable melting as the temperature of the sea-water is seldom above 0° C. However, in conjunction with the outflow of geothermal heat, it is possibly sufficient to raise the temperature of the ice bed to its pressure melting point, facilitating movement of the ice.

d. *Evaporation losses.* The conditions necessary to produce large evaporation losses (warm, dry wind) seldom occur at the Argentine Islands and such losses are small.

e. *Calving.* Apart from the annual removal of winter drift formation, there is little regular calving. The southern ice cliffs of Galindez Island have been known to calve at intervals of from five to ten years.

Net accumulation

The net accumulation varies considerably from year to year (Fig. 9) due mainly to differences in the summer temperatures. In Table II the annual net accumulation at the top of the ice cap is compared with the summer mean temperature for each of the budget years during 1958–63. The cold summer of 1958–59 resulted in relatively little ablation and consequently a large positive value for net accumulation. The high mean summer temperature for 1962–63 resulted from high temperatures in January and February of 1963 which were not, however, sufficiently prolonged to cause considerable ablation. These months were immediately followed by a rapid fall in temperature and there is every indication that the mean temperature for 1963 will be low. The positive budget of 1960–61 resulted from the heavy snow falls during early spring which retarded ablation.

In Fig. 10 the annual mean temperature is plotted against time and the resultant curve shows a marked cyclic form with an approximately five-year period between peaks in the annual mean temperature. The "cold" years also occur at five-year intervals and they are always accompanied by cold summers. It is therefore probable that the budget state at the Argentine Islands also follows a cyclic pattern with large positive values every five years and a slow wasting of the excess accumulation during the intervening warm summers.

The net result of this is difficult to assess, but from a comparison of photographs of the island taken by the British Graham Land Expedition in 1935 with those taken by the writer in 1960 and 1961, it seems probable that the ice cap is in a state of equilibrium, and the large net surface accumulation (of the order of 40 cm. water/yr.) above the southern ice cliffs (stakes 12 and 23) is being removed by forward movement and periodic calving of the cliffs.

The values of snow accumulation shown in Table II indicate that over the four years 1958–62 (one complete temperature variation cycle, assuming 1963 will be a "cold" year) the total net accumulation at the top of the ice cap was +41 cm. water or +10 cm. water/yr., but this value is probably not representative of the budget state, due to the positive budget of 1960–61. This period was preceded by four warm years (1954–57) with a mean annual temperature of −4·0° C and with three very warm summers. These almost certainly resulted in a net ablation during this period of at least the same magnitude as the net accumulation observed during 1958–62. Thus, over a number of years a balance is probably achieved and the height of the ice cap oscillates 1–2 m. about an equilibrium value. In this context it is

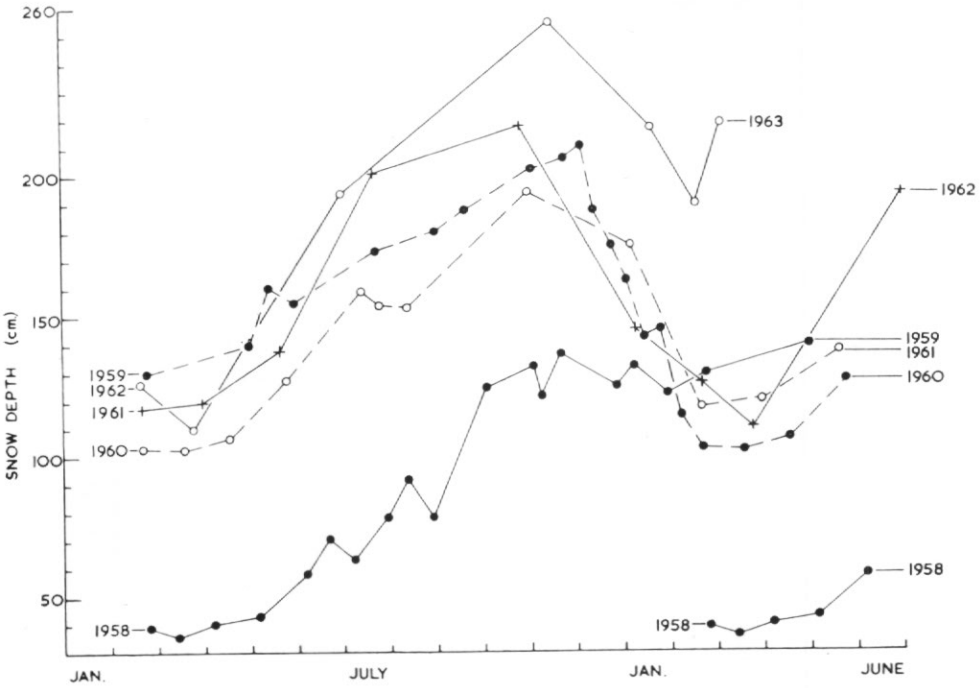

Fig. 9. Variation of snow depth at the top of the Galindez Island ice cap relative to a fixed datum during the period February 1958–March 1963. The values for February 1958–February 1960 were recorded by G. J. Roe using stake 1 (Fig. 2), and those for February 1960–March 1963 were recorded by the writer and A. Schärer using the mean of readings taken at stakes 13 and 14.

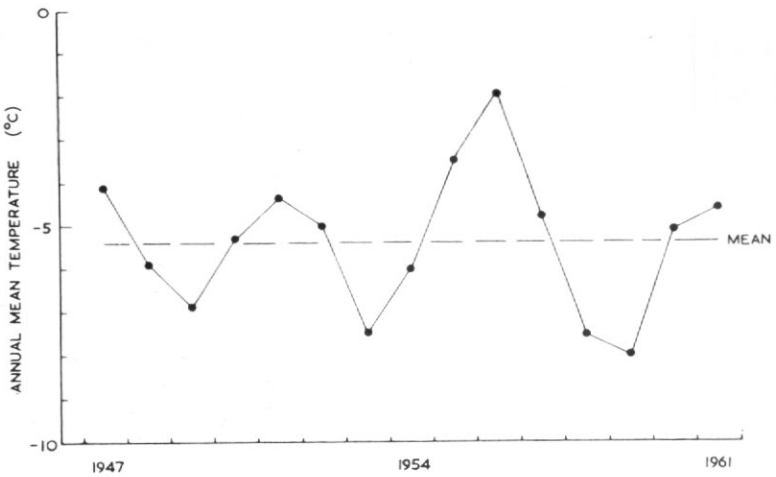

Fig. 10. Variation in annual mean temperature over the period 1947–61.

TABLE II. COMPARISON BETWEEN ANNUAL NET ACCUMULATION ON TOP OF THE ICE CAP AND MEAN SUMMER TEMPERATURES

Budget Year (April–March)	*Annual Net Accumulation* *Snow Depth* (cm.; $\rho = 0{\cdot}63$)	*Water Equivalent* (cm.)	*Mean Summer Temperature for 1 December–31 March* (° C)
1958–59	+85	+54	−1·8
1959–60	−20	−13	+0·4
1960–61	+15	+9	−0·1
1961–62	−15	−9	−0·5
1962–63	+90	+57	−0·5

Total net accumulation for 1958–63 = +98 cm. water.
Mean annual net accumulation = +19·6 cm. water.

interesting to note that the highest point on the Galindez Island ice cap, measured in the summer of 1934–35 by A. Stephenson (Fleming and others, 1938), was 53·9 m. above sea-level, and that the height measured in March 1961 by the writer, using the same datum level, was 54·1 m. above sea-level. Assuming Stephenson's measurements were made at the end of the summer, there has been virtually no change in the height of the ice cap over a period of 26 years.

Distribution of accumulation

In Table III depths of snow above the stake horizons are given for 1 April 1961 and 3 March 1963. Unfortunately stakes 20 and 21 melted out during the 1961–62 summer, but previous observations indicate that accumulation at these sites is low and probably of the order of +50 cm. of snow over the two-year period. Stake 23 was buried by the heavy snowfalls of the 1962 winter and it was not exposed by ablation during the following summer. However, it is estimated (p. 40) that in March 1963 the top of this stake was about 15 cm. beneath the snow surface, due to a net accumulation of about 265 cm. of snow during 1961–63.

Accumulation during the period was very high, due mainly to low ablation in the summer of 1962–63 and to a series of heavy snowfalls during February 1963. Therefore, the values for snow accumulation shown in Table III are greatly in excess of the mean annual net accumulation. However, they give a good picture of the relative accumulation at the stake sites, and the distribution of accumulation over the island is represented in Fig. 2.

The pattern of deposition is mainly determined by the prevailing north-north-east wind and the presence of rock obstructions. The main features are:

i. The heavy accumulation immediately to windward of the north cliff face of Woozle Hill (i.e. stakes A, B and 16 in Fig. 2) is caused by high drift accumulation above the windscoop which exists at the base of the cliff.
ii. Heavy accumulation at stakes 9 and 15 due to local rock obstructions to the north.
iii. Low accumulation at stakes 6A, 10, 20 and 21, due to the scouring effect of wind passing around Woozle Hill. During summer this effect is sufficient to expose the underlying ice. These scouring winds become heavily charged with drift snow and receive an upward velocity component from the slope of the surface over which they pass. The wind velocity accordingly decreases towards the top of the ice cap and much of the drift snow is redeposited southward of stakes 11 and 22.
iv. The phenomenon described above, however, does not fully explain the very high values for snow accumulation at stakes 12 and 23, which are set in the southern fringe of deep firn and separated from the main body of ice by a series of small crevasses. The major crevasses (C_2 and C_3 in Fig. 2) are opening at about 100 cm. $yr.^{-1}$ and the ice to the south is moving downwards at about 80 cm. $yr.^{-1}$.

TABLE III. SNOW DEPTHS ON GALINDEZ ISLAND AND TOTAL NET ACCUMULATION OVER A TWO-YEAR PERIOD

Stake Number		2	3	5	6A	7	9	10	A	B	C	11	12	13	14	15	16	17	20	21	22	23	23A	23B
Snow Depth above Stake Horizon (cm.)	1 April 1961	12	58	69	93	55	84	86	107	67	67	46	167	60	46	17	55	40	18	15	12	167	100	52
	3 March 1963	101	142	162	147	136	191	150	223	180	130	127	381	165	140	138	170	118	?	?	96	>413	203	155
Depth of Snow Accumulated from April 1961 to March 1963 (cm.)		+89	+84	+93	+54	+81	+107	+64	+116	+113	+63	+81	+214	+105	+94	+121	+115	+78	?	?	+84	>+246	+103	+103

Drift snow is therefore preferentially deposited south of crevasses C_2 and C_3 in order to maintain the surface configuration of the ice cap. The difference between the annual net accumulation at stake 12 (A_{12}) and that at stake 11 (A_{11}) is equal to the downward velocity ($\dot{H}_{12}$) of stake 12, because $\dot{H}_{11} = 0$.

For 1961–63, $A_{12} = 107$ cm. snow/yr. and $A_{11} = 40$ cm. snow/yr.

$\dot{H}_{12} = A_{12} - A_{11} = 107 - 40 = 67$ cm. yr.$^{-1}$ (calculated), and

$\dot{H}_{12} = 63$ cm. yr.$^{-1}$ (observed).

For stakes 23 and 23A, where for 1961–63 $A_{23A} = 51$ cm. snow/yr. and $\dot{H}_{23} - \dot{H}_{23A} = 81$ cm. yr.$^{-1}$,

$\dot{H}_{23} - \dot{H}_{23A} = A_{23} - A_{23A}$ and therefore $A_{23} = 51 + 81 = 132$ cm. snow/yr.

Hence for the two years March 1961–March 1963, the net accumulation at stake 23 was approximately 265 cm. of snow, but in March 1961 250 cm. of stake 23 were exposed, indicating that in March 1963 the top of the stake was approximately 15 cm. below the snow surface. This agrees with the observed fact that the stake was buried.

Temperatures in the snow

Snow temperatures plotted against depth below the snow surface are shown in Fig. 6. Unfortunately, there are no values for November–March, but the March temperatures indicate a complete removal of the winter cold wave (the small cold wave present was probably caused by low air temperatures experienced in early March).

The temperature profiles observed in the solid ice (Fig. 6A) show several marked differences from those in the firn (Fig. 6B). Despite better heat conductivity in the ice, the ice temperature is generally lower than that of the firn, and at a depth of 8 m. it reaches an almost constant value of $-4°$ C compared with a value of $-1{\cdot}5°$ C at the same depth in the firn. This is thought to be due to the warming of the firn during summer by latent heat released by refreezing melt water. In May 1961 the firn at a depth of 5 m. was still saturated with summer melt water and the firn temperature was 0° C.

Melt water formed above the solid ice is unable to penetrate beneath the ice surface and freezes to form superimposed ice, the latent heat released being absorbed at the surface of the solid ice and conducted downwards. This process continues until the temperature of the ice surface reaches 0° C and the temperature gradient in the underlying ice is too low for all the released latent heat to be conducted away. The melt water then oversaturates the lower layers of the surface snow, resulting finally in run-off along the ice surface and melting of the superimposed ice. Thereafter, the ice is warmed by conduction of atmospheric heat through the snow cover.

Variations in the thickness of the superimposed ice at several stakes is shown in Fig. 11.

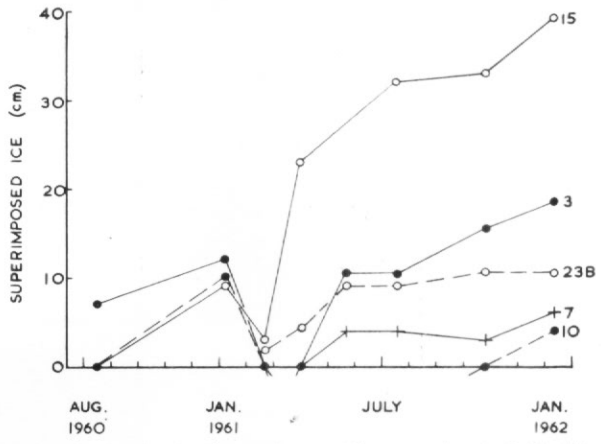

Fig. 11. The seasonal variation in the depth of superimposed ice at stakes 3, 7, 10, 15 and 23B on the Galindez Island ice cap for the period August 1960–January 1962.

Accumulation of ice commences in autumn when the lower layers of saturated snow freeze. At stake 15, situated on a flat surface which retains much of the surface melt water, there is a considerable autumn accumulation of ice. By June, however, thawing is usually not severe enough to enable melt water to penetrate the snow cover and no further superimposed ice is formed until the spring thaws of October/November. It is possible to estimate approximately the amount of melt water refrozen at depth in the spring of 1961: above the solid ice to form superimposed ice, and in the firn.

a. Warming of the ice during the period 20 October–27 November 1961 is assumed to be caused by the release of latent heat at the ice surface; after 27 November the ice surface was at a temperature of 0° C and subsequent warming of the ice (profiles 3 to 1 in Fig. 6A) is assumed to be caused by conduction of atmospheric heat through the snow cover.

If A = The area between profiles 2 and 3 (Fig. 6A) and below the surface of the ice ($= 5{\cdot}6\times10^2$ cm.^{3} ° C per cm.^{2} surface area);
ρ = The average density of the ice;
S = Specific heat of ice ($= 0{\cdot}48$ cal. g.$^{-1}$ ° C^{-1});
L = Latent heat of freezing of water ($= 80$ cal. g.$^{-1}$);
M = Mass of water refrozen per cm.^{2} surface area,

then $ML = A\rho S$, i.e. $M = \dfrac{A\rho S}{L}$,

and $T = \dfrac{M}{\rho} = \dfrac{AS}{L}$, where T = thickness of superimposed ice,

$$= \frac{5{\cdot}6\times10^2\times0{\cdot}48}{80} = 3{\cdot}4 \text{ cm. ice.}$$

The average increase in the thickness of superimposed ice at the five stake sites shown in Fig. 11 was 4 cm., which is in good agreement with the value of 3·4 cm. of ice.

b. The summer temperature profile in the firn (profile 1 in Fig. 6B) indicates that melt water sinks to a depth of 5 to 6 m., and it is assumed that the cold wave (profiles 2 to 1) was removed by the release of latent heat alone.

If A = The area between profiles 2 and 1 (Fig. 6B) and below the base of stake 23 ($= 15\times10^2$ cm.^{3} ° C per cm.^{2} surface area);
ρ = The average density of the firn to a depth of 9 m. ($= 0{\cdot}6$ g. cm.$^{-3}$);
S = Specific heat of ice ($= 0{\cdot}48$ cal. g.$^{-1}$ ° C^{-1});
L = Latent heat of freezing of water ($= 80$ cal. g.$^{-1}$);
M = Mass of water refrozen per cm.^{2} surface area,

then $ML = A\rho S$, i.e. $M = \dfrac{15\times10^2\times0{\cdot}6\times0{\cdot}48}{80} = 5{\cdot}4$ g. cm.$^{-2}$.

This value gives the mass of melt water refrozen during the removal of the winter cold wave, but it does not give a measure of the melt water retained by the firn which is refrozen at the beginning of the winter. Therefore, of the net apparent summer ablation at stakes 12 and 23 (approximately 40 g. cm.$^{-2}$), at least 5 g. cm.$^{-2}$ are refrozen at depth.

Movement

Values for annual movement observed at each stake are shown in Table I. Surface movement on the ice cap is negligible except in the firn situated immediately above, and extending 60 to 80 m. inland from the southern ice cliffs of Galindez Island. This active fringe of ice and firn is separated from the main body of ice by a series of small crevasses (Fig. 2) and much of the surface movement is caused by "opening" of these crevasses. For this reason stakes 23, 23A and 23B have widely differing velocities, although they are only separated by distances of approximately 20 m. The crevasse widths, however, remain almost constant, and this is thought to be due to filling by snow from collapsed bridges, drift accumulation, crevasse hoar formation and spreading of the surrounding firn as it settles.

Mechanism

There are two feasible explanations for the movement observed.

a. Attenuation of the underlying ice by plastic deformation and a resultant forward motion

which increases from approximately zero below stake 23B to about 150 cm. yr.$^{-1}$ at the ice cliff. The overlying firn which is carried along by the ice splits into large blocks, separated by a series of cracks and small crevasses which form perpendicular to the direction of flow.

The downward velocity, $\dot{H}$, at the surface is caused by:

i. Settling of the firn.
ii. Attenuation of the underlying ice as described above.
iii. Downward movement due to the slope of the rock bed beneath the ice cap.

$\dot{H}$ is observed to be approximately equal to the mean annual net accumulation, A, of surface snow above the moving ice, i.e. the surface profile remains the same and the ice cap is in equilibrium.

Consider a 1 cm. thick vertical section of ice and firn taken perpendicular to the ice cliff near stake 23 (Fig. 12). The velocity of stake 23 is assumed to be equal to the velocity of the

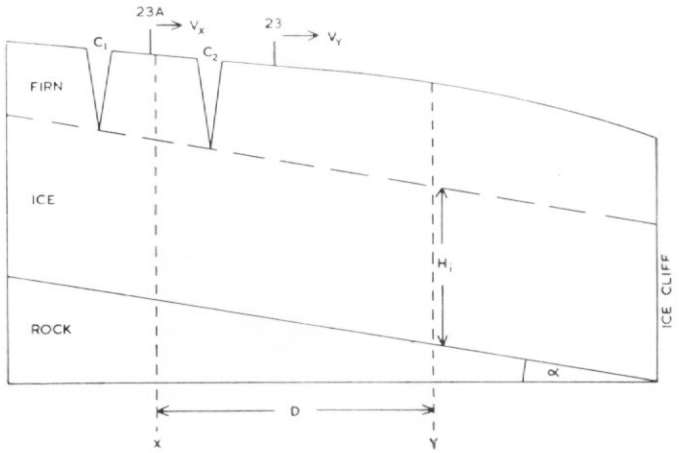

Fig. 12. Vertical section through the Galindez Island ice cap, perpendicular to the southern ice cliffs and through stake 23 (Fig. 2).

underlying ice midway between crevasse C_2 and the ice cliff (Y in Fig. 12), that of stake 23A equal to the velocity of the ice midway between crevasses C_1 and C_2 (X in Fig. 12).

If ρ_A = Density of surface snow + $\dfrac{\text{Weight of water refrozen per cm.}^2 \text{ per yr.}}{\text{Depth of annual net accumulation}}$ ($\simeq 0{\cdot}6$ g. cm.$^{-3}$);

ρ_i = Density of the solid ice ($\simeq 0{\cdot}8$ g. cm.$^{-3}$);
H_i = Vertical thickness of solid ice ($\simeq$ 30 m.);
} Values obtained from observations on the ice cliff.

V_y = Velocity of stake 23 (= 108 cm. yr.$^{-1}$);
V_x = Velocity of stake 23A (= 24 cm. yr.$^{-1}$);
A = Average annual net accumulation along XY ($\simeq$ 90 cm. snow);
D = Horizontal distance from X to Y (= 40 m.);
α = Slope of the bedrock,

for mass balance,

$$(V_y - V_x)H_i = D\,[(A\rho_A/\rho_i) - (V_y - V_x)\tan\alpha], \text{ since } A \simeq \dot{H},$$

$$\text{and } \tan\alpha = \left[\frac{A\rho_A}{\rho_i} - \frac{(V_y - V_x)\,H_i}{D}\right] \Big/ (V_y - V_x)$$

$$= \left[\frac{90\times 0{\cdot}6}{0{\cdot}8} - \frac{84\times 30}{40}\right] \Big/ 84 = 0{\cdot}053.$$

Therefore $\alpha = 3°$.

The probable error in this result is of the order of $\pm 5°$ due mainly to errors in the estimation of H_i. However, it does indicate that, if plastic flow is taking place, the bedrock beneath the moving ice is approximately horizontal as shown in Fig. 2.

If this platform is below the high-tide level, then sea-water could percolate along the bedrock surface, warming the ice and, due to its salt content, lowering the melting point of the ice. Such an effect would considerably reduce the yield shear stress of the ice, and may well explain the fact that movement is confined to the narrow fringe of ice bordering the southern ice cliffs.

b. *En masse* bottom sliding of the ice which, due to irregularities in the bedrock surface, cracks into large roughly rectangular blocks separated by crevasses aligned at right angles to the direction of movement. In moving forward 108 cm., the ice below stake 23 is moving downwards about 65 cm. Therefore, the slope of the bedrock is $\tan^{-1}\frac{65}{108} \simeq 31°$. Such a rock slope would reach the snow surface to the south of stake 23 (Fig. 2) and is considered unlikely. However, it is possible that the bedrock is formed of a series of *roche moutonnées* reaching a peak at station 207. The southernmost of these, shown in the suggested bedrock profiles in Fig. 2, possesses an upstream face sloping at about 15°, a value based on the existing features on neighbouring islands. Ice sliding over such a slope with a forward velocity of 108 cm. yr.$^{-1}$ would move downwards at about 30 cm. yr.$^{-1}$, or about 35 cm. yr.$^{-1}$ less than observed. If bottom sliding is taking place, then it is probable that it occurs in conjunction with plastic deformation of the ice.

ACKNOWLEDGEMENTS

Considerable help was received from personnel at the Falkland Islands Dependencies Survey station on Galindez Island during 1960–61. The results of work done at the Argentine Islands by G. J. Roe (1958–60) and A. Schärer (1962–63) have been used in the compilation of this report, and their work is gratefully acknowledged. Thanks are also due to Dr. R. J. Adie and Dr. J. W. Glen for their helpful criticism and discussion of this work.

MS. received 19 June 1963

REFERENCE

FLEMING, W. L. S., STEPHENSON, A., ROBERTS, B. B. *and* G. C. L. BERTRAM. 1938. Notes on the Scientific Work of the British Graham Land Expedition, 1934–37. *Geogr. J.*, **91**, No. 6, 508–32.